AGU PUBLICATIONS

Paleoceanography

RESEARCH ARTICLE

10.1002/2016PA003049

Key Points:

- Coral delta^{13}C and TSI have significant positive correlation and coupled variation over centennial scales during the MWP and LIA
- Coral delta^{13}C and TSI become decoupled during the CWP around A.D. 1900
- The decoupling of coral delta^{13}C and TSI over centennial scales was caused by the oceanic ^{13}C Suess effect

Correspondence to:
W. Deng,
wfdeng@gig.ac.cn;
wfdeng@gmail.com

Citation:
Deng, W., X. Chen, G. Wei, T. Zeng, and J. Zhao (2017), Decoupling of coral skeletal δ^{13}C and solar irradiance over the past millennium caused by the oceanic Suess effect, *Paleoceanography*, *32*, 161–171, doi:10.1002/2016PA003049.

Received 20 OCT 2016
Accepted 2 FEB 2017
Accepted article online 4 FEB 2017
Published online 17 FEB 2017

Decoupling of coral skeletal δ^{13}C and solar irradiance over the past millennium caused by the oceanic Suess effect

Wenfeng Deng[1], Xuefei Chen[1], Gangjian Wei[1], Ti Zeng[2], and Jian-xin Zhao[3]

[1]State Key Laboratory of Isotope Geochemistry, Guangzhou Institute of Geochemistry, Chinese Academy of Sciences, Guangzhou, China, [2]Key Laboratory of Marginal Sea Geology, Guangzhou Institute of Geochemistry, Chinese Academy of Sciences, Guangzhou, China, [3]Radiogenic Isotope Laboratory, Centre for Microscopy and Microanalysis, University of Queensland, Brisbane, Queensland, Australia

Abstract Many factors influence the seasonal changes in δ^{13}C levels in coral skeletons; consequently, the climatic and environmental significance of such changes is complicated and controversial. However, it is widely accepted that the secular declining trend of coral δ^{13}C over the past 200 years reflects the changes in the additional flux of anthropogenic CO_2 from the atmosphere into the surface oceans. Even so, the centennial-scale variations, and their significance, of coral δ^{13}C before the Industrial Revolution remain unclear. Based on an annually resolved coral δ^{13}C record from the northern South China Sea, the centennial-scale variations of coral δ^{13}C over the past millennium were studied. The coral δ^{13}C and total solar irradiance (TSI) have a significant positive Pearson correlation and coupled variation during the Medieval Warm Period and Little Ice Age, when natural forcing controlled the climate and environment. This covariation suggests that TSI controls coral δ^{13}C by affecting the photosynthetic activity of the endosymbiotic zooxanthellae over centennial timescales. However, there was a decoupling of the coral skeletal δ^{13}C and TSI during the Current Warm Period, the period in which the climate and environment became linked to anthropogenic factors. Instead, coral δ^{13}C levels have a significant Pearson correlation with both the atmospheric CO_2 concentration and δ^{13}C levels in atmospheric CO_2. The correlation between coral δ^{13}C and atmospheric CO_2 suggests that the oceanic ^{13}C Suess effect, caused by the addition of increasing amounts of anthropogenic $^{12}CO_2$ to the surface ocean, has led to the decoupling of coral δ^{13}C and TSI at the centennial scale.

1. Introduction

Scleractinian reef corals are one of the main archives of past climatic and environmental information in the tropical oceans, such as sea surface temperature (SST), sea surface salinity (SSS), and pH [*Felis and Pätzold*, 2003; *Pelejero et al.*, 2005; *Wei et al.*, 2009; *Lough*, 2010; *Liu et al.*, 2014]. However, compared with some other widely used geochemical proxies (such as Sr/Ca, Mg/Ca, and δ^{18}O), the use of coral δ^{13}C as a proxy for environmental and climatic change remains a matter for debate [*Fairbanks and Dodge*, 1979; *Swart*, 1983; *McConnaughey*, 1989, 2003; *Swart et al.*, 1996; *McConnaughey et al.*, 1997; *Grottoli*, 2002]. At the cellular scale, carbon precipitated in coral skeletons originates directly from dissolved inorganic carbon (DIC) in the extracellular calcifying fluid (ECF) that forms an interior pool beneath the calicoblastic layer of coral polyps where the calcification takes place [*Gattuso et al.*, 1999]. Inorganic carbon derived from metabolic respiration inside the coral polyps and external seawater may both contribute to the carbon in the ECF used for calcification, although the relative contribution from these two sources remains unknown [*Furla et al.*, 2000; *Al-Horani et al.*, 2003; *McConnaughey*, 2003]. Therefore, any biological or environmental factor that is able to influence the δ^{13}C levels preserved in these two sources of inorganic carbon input to the ECF would also affect δ^{13}C variations recorded in coral skeletons.

The climatic and environmental implications of seasonal variations in coral δ^{13}C levels are site specific. A number of studies have demonstrated that a wide range of different factors, such as light availability (cloud cover) and water depth [*Land et al.*, 1975; *Weber et al.*, 1976; *Fairbanks and Dodge*, 1979; *Swart et al.*, 1996; *Grottoli and Wellington*, 1999; *Heikoop et al.*, 2000; *Grottoli*, 2002; *Maier et al.*, 2003; *Rosenfeld et al.*, 2003], kinetic isotope fractionation [*McConnaughey*, 1989], the δ^{13}C of DIC in surrounding seawater [*Swart et al.*, 1996; *Watanabe et al.*, 2002; *Moyer and Grottoli*, 2011; *Deng et al.*, 2013a], feeding [*Grottoli*, 2002; *Reynaud et al.*, 2002], spawning [*Gagan et al.*, 1994, 1996], and bleaching [*Porter et al.*, 1989; *Leder et al.*, 1991; *Allison et al.*, 1996], plays important roles in the seasonal variations of coral skeletal δ^{13}C levels.

Compared with the seasonal variations in coral $\delta^{13}C$, the climatic and environmental significance of centennial-scale changes in coral $\delta^{13}C$ is relatively well defined. The secular declining trend in coral $\delta^{13}C$ levels over the past 200 years reflects the increase in the transfer of anthropogenic CO_2 from the atmosphere to the surface oceans [*Swart et al.,* 2010; *Dassié et al.,* 2013]. However, the significance of the long-term variations in coral $\delta^{13}C$ levels before the Industrial Revolution remains unclear, and, to date, comparative studies of the preindustrial and postindustrial periods are still rare [*Druffel and Griffin*, 1993; *Quinn et al.,* 1998]. As the anthropogenic influence on climatic and environmental changes was relatively weak before the Industrial Revolution, anthropogenic CO_2 should have played a limited role in the long-term change of preindustrial coral $\delta^{13}C$ levels. The time series of $\delta^{13}C$ records from coralline sponge skeletons can be subdivided into two parts: a preindustrial period, during which the isotopic composition is controlled by climatic forcings, followed by the Industrial Era, characterized by a progressive enrichment in ^{12}C caused by massive carbon emissions of anthropogenic origin [*Böhm et al.,* 2002; *Madonia and Reitner*, 2014]. The Medieval Warm Period (MWP, A.D. 900–1300) [*Lamb*, 1965; *Crowley and Lowery*, 2000; *Bradley et al.,* 2003] and the Little Ice Age (LIA, A.D. 1550–1850) [*Robock*, 1979; *Bradley and Jones*, 1993; *Matthews and Briffa*, 2005] were climatic and environmental anomalies caused by natural forcing (e.g., solar variability and volcanic emissions). However, the Current Warm Period (CWP, A.D. 1850 to present) [*Wu et al.,* 2012; *Fleury et al.,* 2015] is believed to be driven by anthropogenic factors (e.g., industrialization and land use changes). Therefore, a comparative study of these three contrasting climate intervals may allow us to develop a better understanding of the climatic and environmental significance of the centennial-scale changes in coral $\delta^{13}C$ levels. Here we use five corals from the northern South China Sea (SCS) that lived during the MWP, LIA, and CWP to study the centennial-scale changes in coral $\delta^{13}C$ levels and to provide a new insight into the control mechanism of long-term changes in coral $\delta^{13}C$ before the Industrial Revolution.

2. Materials and Methods

One modern coral and four fossil coral drillcores, with diameters of 0.5–1.5 m, were recovered using an underwater pneumatic drill from five *Porites lutea* colonies in water depths of 4–6 m on the fringing reefs at Qionghai off the coast of eastern Hainan Island in the northern SCS. Hainan Island has an oceanic tropical climate that is controlled by the East Asian monsoon. The summer monsoon runs from May to October and brings warmer and fresher conditions (SST: 27–33°C, SSS: 25–31), while the winter monsoon dominates from November to April and brings colder and saltier conditions (SST: 17–27°C, SSS: 31–33). The modern coral 11LW4 and the fossil coral 11LW2 were collected at Longwan (11LW4: 19°17′11.94″N, 110°39′21.06″E; 11LW2: 19°17′18.84″N, 110°39′23.40″E) in April 2011. The fossil corals 11QG1 and 11QG3 were collected at Qingge (11QG1: 19°18′30.48″N, 110°40′2.46″E; 11QG3: 19°18′3.72″N, 110°39′41.52″E) also in April 2011. The fossil coral 13OC4 was collected at Oucun (19°19′11.22″N, 110°41′31.26″E) in August 2013. The sampling locations are shown in Figure 1. The modern coral 11LW4 (A.D. 1853–2011) has been used previously to study decadal variability in the northern SCS [*Deng et al.,* 2013b; *Chen et al.,* 2015; *Wei et al.,* 2015].

The coral cores were first sectioned into slices 1 cm thick and 5–7 cm wide. Then, X-ray photographs were taken to reveal the regular and well-defined annual density bands, which were used to establish the coral chronology. Next, the coral slices were soaked in 10% H_2O_2 for 24 h to remove organic matter, and this was followed by ultrasonic cleaning in deionized water for 30 min to remove surface contaminants. The 412 subsamples (approximately 0.1 g each) were collected at annual intervals along the main growth axis of each coral using a digitally controlled milling machine. Each high-density and low-density band constitutes an annual couplet, generally representing 1 year of growth [*Knutson et al.,* 1972]. The annual growth rate was directly measured (with a precision of 1 mm) along the major growth axis from the X-ray photograph as the length of each annual density band. X-ray diffraction analysis of the samples showed that the coral skeletons were 100% aragonite. Scanning electron microscopy imaging revealed that there was no secondary aragonite present in the coral skeletons.

The four fossil corals were subjected to U-Th dating using multicollector-inductively coupled plasma-mass spectrometers (MC-ICP-MS) at the Radiogenic Isotope Laboratory of the University of Queensland and at the High-Precision Mass Spectrometry and Environment Change Laboratory of National Taiwan University. A sample of ~0.5 g was taken from the age control point of each fossil coral and spiked with a ^{229}Th-^{233}U mixed tracer. The detailed analytical methods and the correction protocols used for the ^{230}Th ages can be

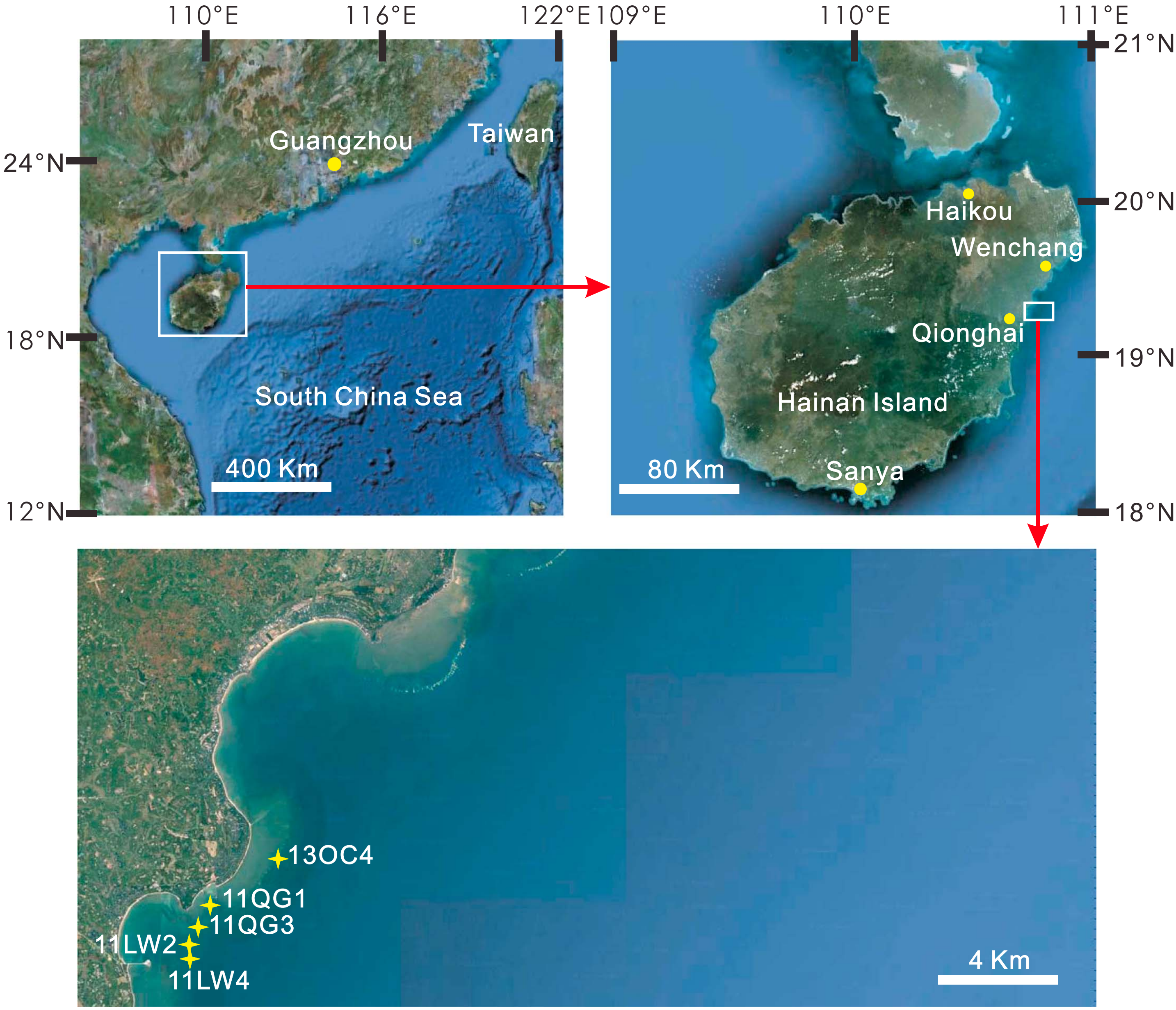

Figure 1. Satellite image of Hainan Island and the northern SCS. Yellow stars indicate sampling locations.

found in *Clark et al.* [2014]. The chronology of the fossil coral was established by counting the annual bands back and forth from the U-Th dated calendar year of the age control point. For the modern coral, the chronology was established by counting the annual bands back from the youngest band, which represents the year of sampling.

The coral skeletal $\delta^{13}C$ and $\delta^{18}O$ analysis was performed using a GV Isoprime II stable isotope ratio mass spectrometer coupled with a MultiPrep carbonate device that used 102% H_3PO_4 at 90°C to extract CO_2 from the coral samples and following the procedures described by *Deng et al.* [2009]. Isotope data were normalized against the Vienna Pee Dee Belemnite using the NBS-19 standard ($\delta^{13}C = 1.95‰$, $\delta^{18}O = -2.20‰$). Multiple measurements ($n = 80$) on this standard yielded a standard deviation of 0.03‰ for $\delta^{13}C$ and 0.06‰ for $\delta^{18}O$. Replicate measurements were made on approximately 15% of the samples.

3. Results

We obtained similar annual growth rates (12–15 mm/yr) for the modern and fossil corals. Coral samples 11QG1, 11QG3, 11LW2, and 13OC4 were dated to 756 ± 9.6, 929 ± 24, 371 ± 18, and 254 ± 4 yr B.P., respectively (Table 1). The dated ages of these fossil corals (11QG1, 11QG3, 11LW2, and 13OC4) were transformed into Common Era years, and their growing intervals span approximately A.D. 1129–1255, A.D. 1063–1087, A.D. 1628–1657, and A.D. 1702–1772, respectively. Including the modern coral 11LW4, the lifespans of our coral samples cover the MWP (11QG1 and 11QG3), LIA (11LW2 and 13OC4), and CWP (11LW4).

The annual $\delta^{13}C$ levels obtained from the five corals (Figure 2) ranged from −3.31‰ to −1.82‰, with an average value of −2.38‰, and displayed a gradually increasing trend between A.D. 1063 and A.D. 1087. The long-term variations in coral $\delta^{13}C$ are relatively stable over the period A.D. 1129–1255, with a range from −1.88‰ to −0.55‰ and an average value of −1.24‰. There is a gradual decrease in coral $\delta^{13}C$ between A.D. 1628 and A.D. 1657, which varies between −1.47‰ and −2.79‰ with an average value of −2.13‰ over this period. The variation range of coral $\delta^{13}C$ over the period A.D. 1702–1772 is −3.04‰ to −1.56‰ with an average of −2.31‰. As for the period A.D. 1853–2011, the coral $\delta^{13}C$ follows a remarkable declining trend and varies between −1.12‰ and −3.37‰ with an average of −2.04‰.

The average $\delta^{13}C$ values for the periods A.D. 1063–1087 and A.D. 1702–1772 are statistically significantly lower (at the 0.05 level) than the average during the period A.D. 1853–2011 ($t = -3.61$, $df = 182$, $p = 0.0002$ for A.D. 1063–1087 and A.D. 1853–2011; $t = 4.63$, $df = 228$, $p < 0.00001$ for A.D. 1702–1772 and A.D. 1853–2011). However, the average $\delta^{13}C$ value for the period A.D. 1129–1255 is statistically significantly higher (at the 0.05 level) than that during the period A.D. 1853–2011 ($t = -17.9$, $df = 284$, $p < 0.00001$). The average values for the periods A.D. 1628–1657 and A.D. 1853–2011 are not statistically significantly different at the 0.05 level ($t = -1.06$, $df = 187$, $p = 0.15$).

4. Discussion

4.1. Coral Skeletal $\delta^{13}C$ and Atmospheric CO_2

The anthropogenic release of CO_2 depleted in ^{13}C from the burning of fossil fuels and deforestation has led to a decline of $\delta^{13}C$ levels in atmospheric CO_2 [*Keeling*, 1979; *Friedli et al.,* 1986]. This decrease affects the surface oceanic $\delta^{13}C$ of DIC via the atmosphere-ocean exchange of CO_2 and is recognized as the oceanic $\delta^{13}C$ Suess effect [*Böhm et al.,* 1996]. The centennial-scale variations in coral $\delta^{13}C$ over the past 200 years are thought to be controlled by changes in the amount of anthropogenic CO_2 released into the atmosphere and the ^{13}C Suess effect [*Swart et al.,* 2010]. Therefore, in this study, we used atmospheric CO_2 data to conduct a comparative study of variations in $\delta^{13}C$ levels preserved in corals over the three climate intervals outlined above. We obtained a record of atmospheric CO_2 concentrations with annual to decadal resolutions over the period A.D. 1005–2011 derived from ice core data from http://scrippsco2.ucsd.edu/data/atmospheric_co2 [*Keeling et al.,* 2001] and transformed it to an annual resolution by linear interpolation. The $\delta^{13}C$ levels in atmospheric CO_2 with annual to decadal resolutions over the period A.D. 1006–1993 were extracted from Antarctic ice cores and firn samples [*Francey et al.,* 1999] and transformed to an annual resolution by linear interpolation. Both the atmospheric CO_2 concentration and the $\delta^{13}C$ in atmospheric CO_2 remained relatively stable during the MWP and the LIA, and this stability persisted until about A.D. 1800. Since then, the atmospheric CO_2 concentration has followed a remarkable increasing trend, while the $\delta^{13}C$ levels in atmospheric CO_2 have shown a rapid decline (Figure 3). The variations in coral $\delta^{13}C$ do not match exactly the variations in atmospheric CO_2 concentration or the $\delta^{13}C$ in atmospheric CO_2 during the MWP and LIA. However, the coral $\delta^{13}C$ has followed a persistent declining trend since 1853 during the CWP (Figure 3). In addition, the coral $\delta^{13}C$ has a significant Pearson correlation with the atmospheric CO_2 concentration ($r = -0.47$, $n = 159$, $p < 0.0001$; Figure 4a) and also with the $\delta^{13}C$ in atmospheric CO_2 ($r = 0.37$, $n = 141$, $p < 0.0001$; Figure 4b) since 1853. The sea surface temperature and hydrological conditions during the MWP were closely comparable to those of the CWP, but the LIA was much colder and drier than the CWP in the northern SCS [*Deng et al.,* 2016]. The climatic and environmental anomalies during these two periods were caused by natural forcing, and the atmospheric CO_2 concentration and $\delta^{13}C$ levels in atmospheric CO_2 remained relatively stable because there was no oceanic Suess effect. Therefore, coral $\delta^{13}C$ levels during these two periods were not related to changes in atmospheric CO_2. However, since the Industrial Revolution, the increase in the transfer of anthropogenic $^{12}CO_2$

Table 1. Results of MC-ICP-MS U-Th Dating of the Fossil Corals[a]

Sample Name	U (ppm)	±2σ	^{232}Th (ppb)	±2σ	^{230}Th/^{232}Th	±2σ	^{230}Th/^{238}U	±2σ	^{234}U/^{238}U	±2σ	Uncorrected ^{230}Th Age (a)	±2σ	Corrected ^{230}Th Age (a)	±2σ	Initial ^{234}U/^{238}U	±2σ
11QG1[b]	2.4653	0.0020	1.732	0.007	189.8	1.40	0.008077	0.000052	1.1461	0.0013	772.2	5.1	756	10	1.1464	0.0013
11QG3[b]	2.8684	0.0025	20.052	0.017	26.90	0.42	0.011391	0.000173	1.1464	0.0015	1090.3	16.7	929	24	1.1467	0.0015
11LW2[b]	2.6722	0.0023	14.499	0.013	15.80	0.41	0.005192	0.000134	1.1458	0.0014	495.9	12.9	371	18	1.1459	0.0014
13OC4[c]	2.6771	0.0009	0.247	0.001	88.31	1.26	0.002687	0.000037	1.1449	0.0015	256.6	3.5	254	4	1.1450	0.0015

[a]Ratios are activity ratios calculated from atomic ratios using the decay constants of *Cheng et al.* [2000]. All values have been corrected for laboratory procedural blanks. Uncorrected ^{230}Th age (a) was calculated using the Isoplot/EX 3.0 program [*Ludwig*, 2003], where "a" denotes years. Nonradiogenic ^{230}Th correction was applied assuming that nonradiogenic ^{230}Th/^{232}Th $= 4.4 \pm 2.2 \times 10^{-6}$ (bulk Earth value) and that ^{238}U, ^{234}U, ^{232}Th, and ^{230}Th are in secular equilibrium. Nonradiogenic ^{230}Th correction results in large age error magnification for samples with low ^{230}Th/^{232}Th ratios.

[b]Dates determined at the High-Precision Mass Spectrometry and Environment Change Laboratory, National Taiwan University.

[c]Dates determined at the Radiogenic Isotope Laboratory, University of Queensland.

emissions into the surface ocean led to the ^{13}C Suess effect and the decrease of δ^{13}C in seawater DIC, which caused the secular decline of coral δ^{13}C during the CWP. The decline in coral δ^{13}C does not neatly follow the declines in atmospheric CO_2 concentrations and the δ^{13}C of atmospheric CO_2, but there are decadal-scale changes in coral δ^{13}C during the CWP (Figure 3). This mismatch may reflect the effect of the Pacific Decadal Oscillation, a pattern of interdecadal climate variability that affects the SCS [*Deng et al.*, 2013b].

4.2. Coral Skeletal δ^{13}C and Total Solar Irradiance

The prevailing opinion regarding the control mechanism of coral skeletal δ^{13}C is that increasing the rate of endosymbiotic zooxanthellae photosynthesis may induce an increase in skeletal δ^{13}C [*Swart et al.*, 1996; *McConnaughey et al.*, 1997]. In general, photosynthesis by endosymbiotic zooxanthellae preferentially consumes $^{12}CO_2$, resulting in ^{13}C enrichment of the DIC in the internal calcification pool. Increased solar irradiance may enhance the activity of photosynthesis, thereby resulting in higher δ^{13}C levels in the coral skeleton [*Weil et al.*, 1981; *Grottoli and Wellington*, 1999]. Therefore, we compared two sets of total solar irradiance (TSI) data with the coral δ^{13}C. One set of TSI data with annual to decadal resolutions for the period A.D. 1004–1961 was reconstructed from the fluctuations of cosmogenic nuclides (ftp://ftp.ncdc.noaa.gov/pub/data/paleo/climate_forcing/solar_variability/bard_irradiance.txt) [*Bard et al.*, 2000] and was transformed to an annual resolution by linear interpolation. As this TSI data set ends in A.D. 1961, another TSI data set covering the period A.D. 1000–2003 was reconstructed using a physical model (http://vizier.cfa.harvard.edu/viz-bin/VizieR?-source=J/A+A/531/A6) [*Vieira et al.*, 2011]. The evolution of TSI over the Holocene was estimated using the Spectral And Total Irradiance REconstruction models, employing the basic assumption that variations in solar irradiance are caused by the evolution of the dark and bright magnetic features on the solar surface [*Vieira et al.*, 2011]. The δ^{13}C levels in the coral skeletons closely follow the changes in TSI derived from the cosmogenic nuclides during the MWP and the LIA, but a decoupling occurs around A.D. 1900–1961 during the CWP (Figure 5a). This decoupling also appears between the coral δ^{13}C and TSI records based on the model results during the CWP (Figure 5b). TSI shows a remarkable increase from about A.D. 1900 to 2003 (Figure 5b). In contrast, coral δ^{13}C levels began to decline from around A.D. 1900 onward, and this decreasing trend persisted until 2011. The covariations between the coral δ^{13}C and the modeled TSI during the MWP and the LIA are not as well defined as those between the coral δ^{13}C and TSI trends derived from the cosmogenic nuclides (Figure 5), which may be the result of the different methods of TSI reconstruction used. The coral δ^{13}C has a significant positive Pearson correlation with the nuclide-based TSI during the MWP and the LIA ($r = 0.68$, $n = 253$, $p < 0.0001$; Figure 6a). However, the coral δ^{13}C and TSI show a negative Pearson correlation during the CWP, and this correlation is also

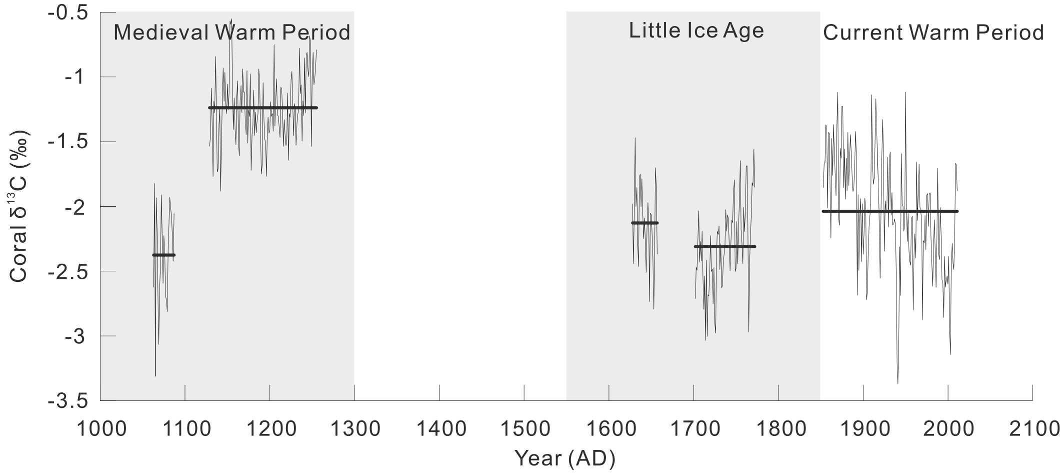

Figure 2. Temporal variations of coral $\delta^{13}C$ during the MWP, LIA, and CWP. Black horizontal lines indicate the average coral $\delta^{13}C$ for different periods. Grey shading indicates the different periods.

significant ($r = -0.25$, $n = 109$, $p = 0.004$; Figure 6b). On the other hand, the results of the spectral analysis performed on the detrended nuclide-based TSI and coral $\delta^{13}C$ time series confirm that the low-frequency trends/variations became decoupled from the 1850s to the present. The power spectrum of the detrended nuclide-based TSI series shows an 86 year cycle that is significant at the 95% confidence level. In contrast,

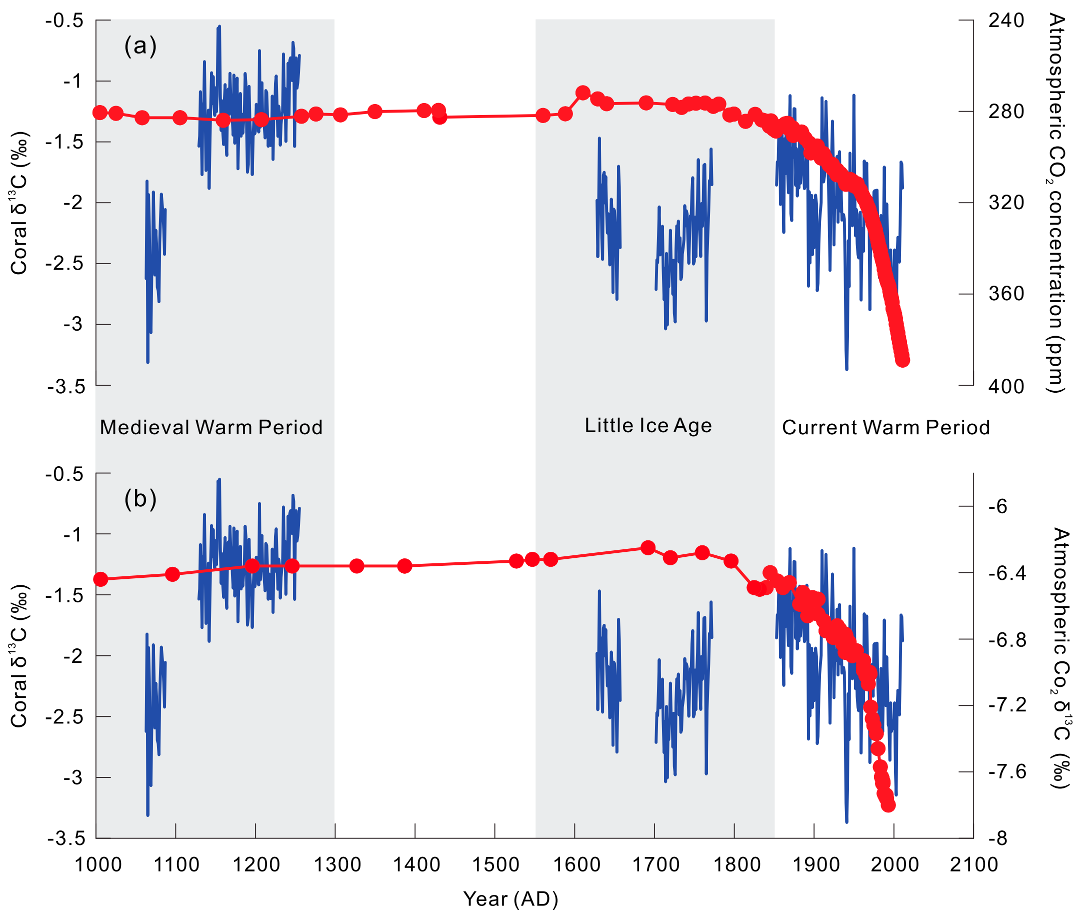

Figure 3. (a) Temporal variations of coral $\delta^{13}C$ (blue lines) and atmospheric CO_2 concentration (red circles with lines, plotted on an inverted scale on the *y* axis) [*Keeling et al.,* 2001] and (b) $\delta^{13}C$ in atmospheric CO_2 (red circles with lines) [*Francey et al.,* 1999] during the MWP, LIA, and CWP.

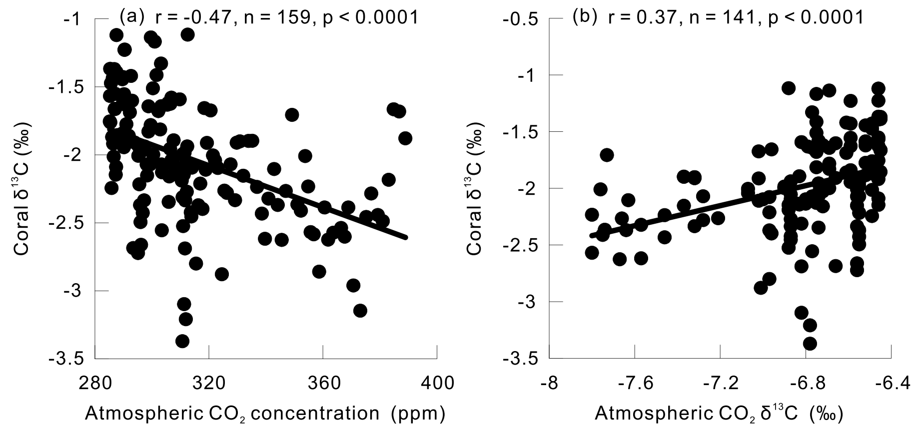

Figure 4. Pearson correlations between coral $\delta^{13}C$ and (a) atmospheric CO_2 concentration [*Keeling et al.,* 2001] and (b) $\delta^{13}C$ in atmospheric CO_2 [*Francey et al.,* 1999] during the CWP.

the power spectrum of the detrended coral $\delta^{13}C$ shows higher-frequency cyclicity with periods of only 15 and 2–7 years [*Deng et al.,* 2013b]. Our observations suggest a coupled variation between coral $\delta^{13}C$ and TSI at the centennial scale; therefore, the changes in coral $\delta^{13}C$ were driven mainly by changes in the photosynthetic activity of the endosymbiotic zooxanthellae associated with TSI at the centennial scale during the MWP and the LIA. However, this coupling was interrupted by the onset of the Industrial Revolution. Considering the significant correlation between the coral $\delta^{13}C$ and atmospheric CO_2 during the CWP, it is reasonable to

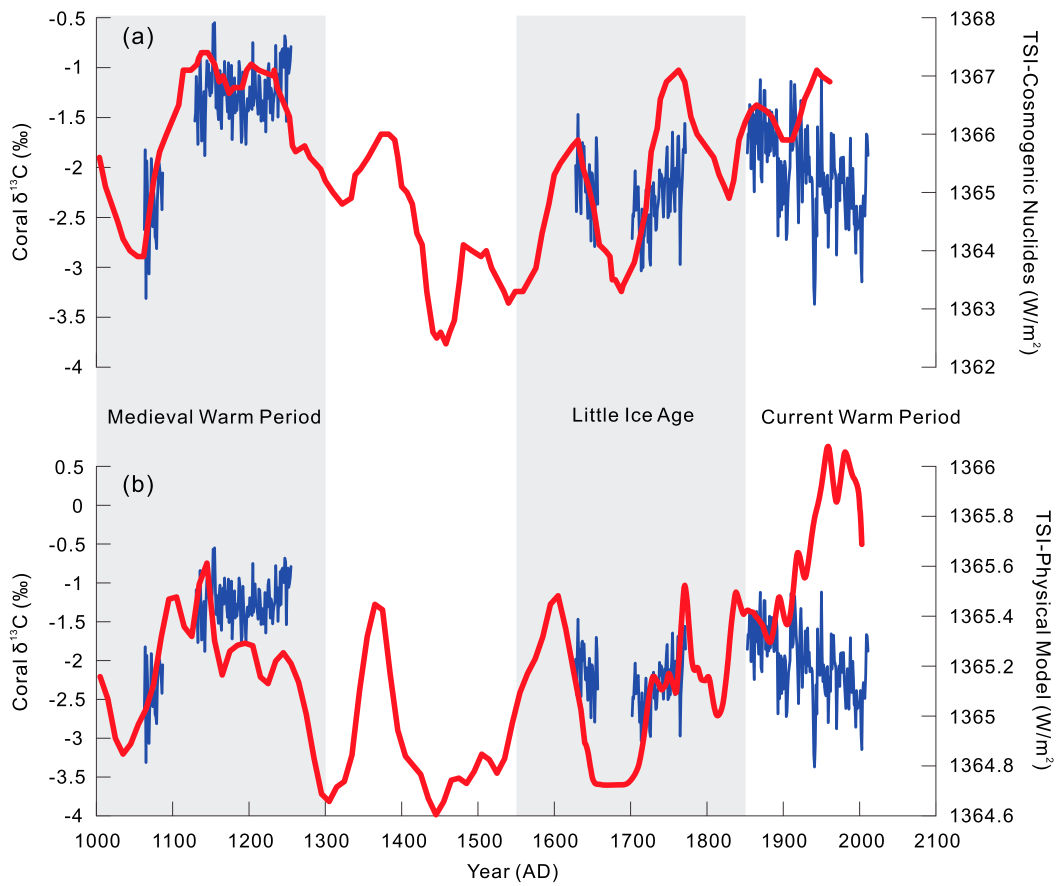

Figure 5. Temporal variations of coral $\delta^{13}C$ (blue lines) and TSI (red lines) reconstructed using (a) cosmogenic nuclides [*Bard et al.,* 2000] and (b) a physical model [*Vieira et al.,* 2011] during the MWP, LIA, and CWP.

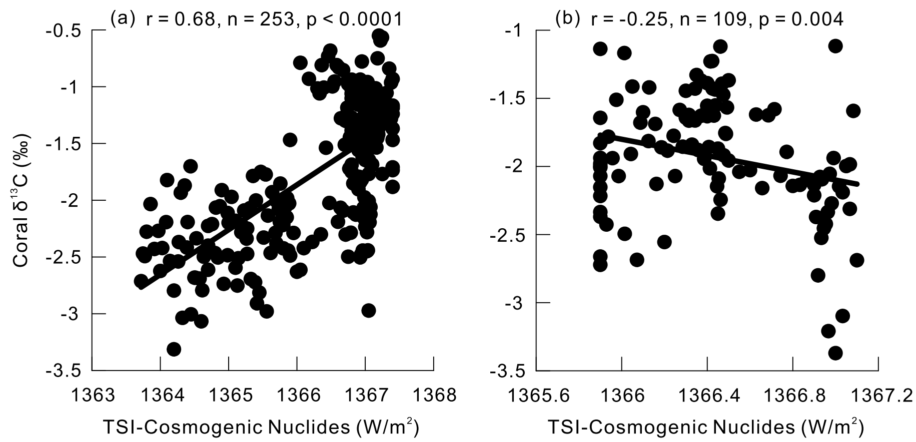

Figure 6. Pearson correlations between coral $\delta^{13}C$ and TSI based on cosmogenic nuclides [*Bard et al.,* 2000] during (a) the MWP and LIA and (b) the CWP.

infer that this decoupling was driven by the oceanic Suess effect. The negative correlation between the coral $\delta^{13}C$ and TSI during the CWP may be an artifact caused by the Suess effect. We note that the average coral $\delta^{13}C$ levels during the periods A.D. 1063–1087 and A.D. 1702–1772 in the MWP and LIA are statistically significantly lower (at a significance level of 0.05) than the average for the period A.D. 1853–2011 during the CWP. These lower coral $\delta^{13}C$ levels were the result of the reduced TSI rather than the oceanic Suess effect caused by the atmosphere-ocean exchange of CO_2.

It is should be noted that the changes in global TSI are small (approximately 3–4 W/m^2) and those in coral $\delta^{13}C$ are large (approximately 2‰), with more irradiance occurring during times of more positive $\delta^{13}C$. The TSI change during the 11 year sunspot cycle is ~1.4 W/m^2, which accounts for ~50% of the TSI signal estimated from the nuclide data and the physical model (Figure 5). It remains unclear why such small changes in irradiance cause such large (2‰) changes in coral $\delta^{13}C$, but the intrinsic "vital effect" within the biomineralization process could be a possible alternative point from which to explore the underlying mechanism.

4.3. Effects of Other Possible Factors on Coral Skeletal $\delta^{13}C$

Although we found good agreement between the coral $\delta^{13}C$ and the TSI during the MWP and the LIA, we must also consider some of the other factors (as outlined in section 1) that affect coral $\delta^{13}C$. For example, there has been a significant amount of discussion regarding kinetic fractionation related to changes in growth rate. *McConnaughey* [1989] suggested that corals with annual growth rates of less than 4 mm/yr may be unsuitable for stable isotopic analysis as these corals would suffer from high levels of isotopic disequilibrium. However, another study found no relationship between growth rate or calcification and skeletal $\delta^{13}C$ in experimental corals [*Swart et al.,* 1996]. Corals growing as slowly as 1.5 mm/yr had essentially identical $\delta^{13}C$ values to portions of the same coral growing at rates of up to 8 mm/yr [*Swart et al.,* 1996]. In the present study, the averaged coral $\delta^{13}C$ values show no relationship with the growth rates of five corals ($r = -0.11$, $n = 5$, $p = 0.43$; Figure 7a). Therefore, the effect of growth rate on the $\delta^{13}C$ levels of the corals studied here may be limited, because their growth rates were similar in all cases and the correlations between coral $\delta^{13}C$ and growth were not statistically significant.

Water depth is another important factor that should be considered because the rates of photosynthesis of endosymbiotic zooxanthellae are higher in shallow-water corals [*Weber et al.,* 1976; *Land et al.,* 1977]. Our coral samples were all collected from water depths of 4–6 m on shallow-water fringing reefs, so any depth-related differences between the $\delta^{13}C$ levels of the different corals can probably be ruled out. To test this assumption, Pearson correlation analysis between the averaged coral $\delta^{13}C$ values of the different periods and the water depths in which the corresponding corals grew was also performed, and the correlation was not significant ($r = 0.19$, $n = 5$, $p = 0.38$; Figure 7b). Therefore, the effect of water depth among the five corals studied here can be ignored.

Previous studies have indicated that circulation changes in the southwestern Pacific played a major role in the large variations in surface ocean radiocarbon via the shoaling of the thermocline or advection of ^{14}C-

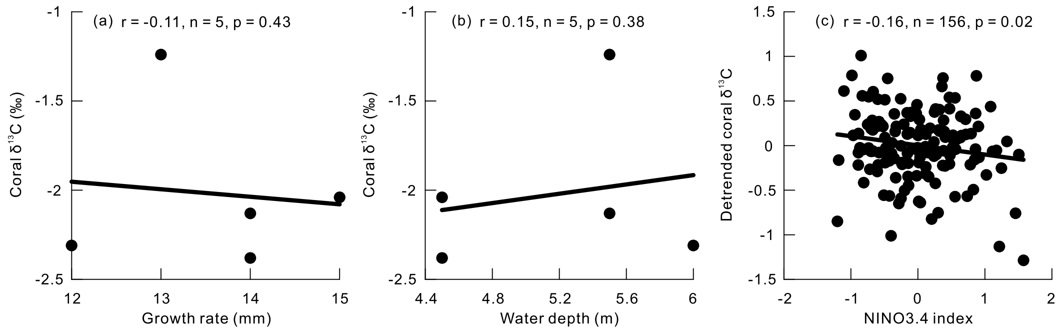

Figure 7. Pearson correlations between coral $\delta^{13}C$ and possible affecting factors. (a) Averaged coral $\delta^{13}C$ values and growth rates of five corals. (b) Averaged coral $\delta^{13}C$ values and the water depths in which the corresponding five corals grew. (c) Detrended coral $\delta^{13}C$ during A.D. 1853–2011 and the NINO3.4 index [*Kaplan et al.,* 1998; *Reynolds et al.,* 2002].

depleted source waters to the southern Great Barrier Reef [*Druffel and Griffin*, 1993]. This indicates that the atmospheric and oceanic circulation should not be ignored as a possible driver of changes in $\delta^{13}C$ level. Circulation variability in the SCS is remotely influenced by El Niño–Southern Oscillation (ENSO) [*Wang et al.,* 2006]; therefore, we compared the NINO3.4 index with the coral $\delta^{13}C$ series to explore the possible effect of ENSO on the latter. The NINO3.4 index is represented by the averages of the monthly SST anomalies during each year in the area bounded by 5°S–5°N, 120°W–170°W from 1856 to the present (http://climexp.knmi.nl/getindices.cgi?WMO=NCEPData/nino5&STATION=NINO3.4&TYPE=i&id=someone@somewhere) [*Kaplan et al.,* 1998; *Reynolds et al.,* 2002]. The correlation between the detrended coral $\delta^{13}C$ series over the period A.D. 1853–2011 and the NINO3.4 index is statistically significant ($r = -0.16$, $n = 156$, $p = 0.02$; Figure 7c) and indicates that only 2.56% (r^2) of the variability in modern coral $\delta^{13}C$ can be accounted for by the NINO3.4 index (i.e., the atmospheric and oceanic circulation). Therefore, the remaining 97.44% of the variability cannot be accounted for by circulation changes, so the latter is unlikely to be one of the main factors influencing coral $\delta^{13}C$ in the SCS. Moreover, the NINO3.4 index is not available for the MWP and LIA, meaning that the effect of atmospheric and oceanic circulation on coral $\delta^{13}C$ levels before the Industrial Revolution remains difficult to evaluate.

5. Conclusions

In this paper, we used an annual-resolution coral $\delta^{13}C$ record from the northern SCS to study centennial-scale variations in coral $\delta^{13}C$ over the past millennium. The coral $\delta^{13}C$ and TSI showed a significant positive Pearson correlation and coupled variation during the MWP and LIA, when the climate and environment were controlled by natural forcing. This covariation suggests that TSI controls coral skeletal $\delta^{13}C$ levels by affecting the photosynthetic activity of the endosymbiotic zooxanthellae at the centennial scale. However, there was a decoupling of the coral skeletal $\delta^{13}C$ from TSI around A.D. 1900 (during the CWP) by which time the climate and environment had become linked by anthropogenic factors. From then on, coral skeletal $\delta^{13}C$ levels have shown a significant Pearson correlation both with the atmospheric CO_2 concentration and with the $\delta^{13}C$ of atmospheric CO_2. The correlations between coral $\delta^{13}C$ and atmospheric CO_2 suggest that the oceanic ^{13}C Suess effect caused by the addition of anthropogenic $^{12}CO_2$ to the surface ocean led to the decoupling of coral $\delta^{13}C$ and TSI at the centennial scale.

Acknowledgments
The authors thank Yi Liu of the University of Science and Technology of China for his assistance with the U-Th dating measurements in the National Taiwan University. The authors would like to thank Editor Heiko Pälike, Associate Editor Elisabeth Sikes, and three anonymous reviewers for their helpful comments and constructive suggestions. The English of the manuscript was improved by Stallard Scientific Editing. This work was supported by the National Key Research and Development Project of China (2016YFA0601204 and 2013CB956103), the National Natural Sciences Foundation of China (41673115 and 41325012), and the State Key Laboratory of Isotope Geochemistry (SKLIG-RC-14-02). This research has made use of the VizieR catalogue access tool, CDS, Strasbourg, France. The original description of the VizieR service was published in A&AS 143, 23. This is contribution IS-2342 from GIGCAS. The data for this paper are available as the online supporting data set and from the corresponding author Deng (wfdeng@gmail.com, wfdeng@gig.ac.cn).

References

Al-Horani, F. A., S. M. Al-Moghrabi, and D. de Beer (2003), The mechanism of calcification and its relation to photosynthesis and respiration in the scleractinian coral *Galaxea fascicularis*, *Mar. Biol.*, *142*(3), 419–426.

Allison, N., A. W. Tudhope, and A. E. Fallick (1996), Factors influencing the stable carbon and oxygen isotopic composition of *Porites lutea* coral skeletons from Phuket, South Thailand, *Coral Reefs*, *15*(1), 43–57.

Bard, E., G. Raisbeck, F. Yiou, and J. Jouzel (2000), Solar irradiance during the last 1200 years based on cosmogenic nuclides, *Tellus B*, *52*(3), 985–992.

Böhm, F., M. M. Joachimski, H. Lehnert, G. Morgenroth, W. Kretschmer, J. Vacelet, and W. C. Dullo (1996), Carbon isotope records from extant Caribbean and South Pacific sponges: Evolution of $\delta^{13}C$ in surface water DIC, *Earth Planet. Sci. Lett.*, *139*(1), 291–303.

Böhm, F., A. Haase-Schramm, A. Eisenhauer, W. C. Dullo, M. M. Joachimski, H. Lehnert, and J. Reitner (2002), Evidence for preindustrial variations in the marine surface water carbonate system from coralline sponges, *Geochem. Geophys. Geosyst.*, *3*(3), 1–13, doi:10.1029/2001GC000264.

Bradley, R. S., and P. D. Jones (1993), "Little Ice Age" summer temperature variations: Their nature and relevance to recent global warming trends, *Holocene*, *3*(4), 367–376.

Bradley, R. S., M. K. Hughes, and H. F. Diaz (2003), Climate in Medieval Time, *Science*, *302*(5644), 404–405.

Chen, X. F., G. J. Wei, W. F. Deng, Y. Liu, Y. L. Sun, T. Zeng, and L. H. Xie (2015), Decadal variations in trace metal concentrations on a coral reef: Evidence from a 159 year record of Mn, Cu, and V in a *Porites* coral from the northern South China Sea, *J. Geophys. Res. Oceans*, *120*, 405–416, doi:10.1002/2014JC010390.

Cheng, H., R. L. Edwards, J. Hoff, C. D. Gallup, D. A. Richards, and Y. Asmerom (2000), The half-lives of uranium-234 and thorium-230, *Chem. Geol.*, *169*(1–2), 17–33.

Clark, T. R., J. X. Zhao, G. Roff, Y. X. Feng, T. J. Done, L. D. Nothdurft, and J. M. Pandolfi (2014), Discerning the timing and cause of historical mortality events in modern *Porites* from the Great Barrier Reef, *Geochim. Cosmochim. Acta*, *138*, 57–80.

Crowley, T. J., and T. S. Lowery (2000), How warm was the Medieval Warm Period? *Ambio*, *29*(1), 51–54.

Dassié, E. P., G. M. Lemley, and B. K. Linsley (2013), The Suess effect in Fiji coral $\delta^{13}C$ and its potential as a tracer of anthropogenic CO_2 uptake, *Palaeogeogr. Palaeoclimatol. Palaeoecol.*, *370*, 30–40.

Deng, W. F., G. J. Wei, X. H. Li, K. F. Yu, J. X. Zhao, W. D. Sun, and Y. Liu (2009), Paleoprecipitation record from coral Sr/Ca and $\delta^{18}O$ during the mid Holocene in the northern South China Sea, *Holocene*, *19*(6), 811–821.

Deng, W. F., G. J. Wei, L. H. Xie, and K. F. Yu (2013a), Environmental controls on coral skeletal $\delta^{13}C$ in the northern South China Sea, *J. Geophys. Res. Biogeosci.*, *118*, 1359–1368, doi:10.1002/jgrg.20116.

Deng, W. F., G. J. Wei, L. H. Xie, T. Ke, Z. B. Wang, T. Zeng, and Y. Liu (2013b), Variations in the Pacific Decadal Oscillation since 1853 in a coral record from the northern South China Sea, *J. Geophys. Res. Oceans*, *118*, 2358–2366, doi:10.1002/jgrc.20180.

Deng, W. F., X. Liu, X. F. Chen, G. J. Wei, T. Zeng, L. H. Xie, and J.-x. Zhao (2016), A comparison of the climates of the Medieval Climate Anomaly, Little Ice Age, and Current Warm Period reconstructed using coral records from the northern South China Sea, *J. Geophys. Res. Oceans*, *121*, xx–xx, doi:10.1002/2016JC012458.

Druffel, E. R. M., and S. Griffin (1993), Large variations of surface ocean radiocarbon: Evidence of circulation changes in the southwestern Pacific, *J. Geophys. Res.*, *98*(C11), 20,249–20,259, doi:10.1029/93JC02113.

Fairbanks, R. G., and R. E. Dodge (1979), Annual periodicity of the $^{18}O/^{16}O$ and $^{13}C/^{12}C$ ratios in the coral *Montastrea annularis*, *Geochim. Cosmochim. Acta*, *43*(7), 1009–1020.

Felis, T., and J. Pätzold (2003), Climate records from corals, in *Marine Science Frontiers for Europe*, edited by G. Wefer, F. Lamy, and F. Mantoura, pp. 11–27, Springer Berlin.

Fleury, S., P. Martinez, X. Crosta, K. Charlier, I. Billy, V. Hanquiez, T. Blanz, and R. R. Schneider (2015), Pervasive multidecadal variations in productivity within the Peruvian Upwelling System over the last millennium, *Quat. Sci. Rev.*, *125*, 78–90.

Francey, R. J., C. E. Allison, D. M. Etheridge, C. M. Trudinger, I. G. Enting, M. Leuenberger, R. L. Langenfelds, E. Michel, and L. P. Steele (1999), A 1000-year high precision record of $\delta^{13}C$ in atmospheric CO_2, *Tellus B*, *51*(2), 170–193.

Friedli, H., H. Lotscher, H. Oeschger, U. Siegenthaler, and B. Stauffer (1986), Ice core record of the $^{13}C/^{12}C$ ratio of atmospheric CO_2 in the past two centuries, *Nature*, *324*(6094), 237–238.

Furla, P., D. Allemand, and M. N. Orsenigo (2000), Involvement of H^+-ATPase and carbonic anhydrase in inorganic carbon uptake for endosymbiont photosynthesis, *Am. J. Physiol.-Regul. Integr. Comp. Physiol.*, *278*(4), R870–R881.

Gagan, M. K., A. R. Chivas, and P. J. Isdale (1994), High-resolution isotopic records from corals using ocean temperature and mass-spawning chronometers, *Earth Planet. Sci. Lett.*, *121*(3–4), 549–558.

Gagan, M. K., A. R. Chivas, and P. J. Isdale (1996), Timing coral-based climatic histories using ^{13}C enrichments driven by synchronized spawning, *Geology*, *24*(11), 1009–1012.

Gattuso, J. P., D. Allemand, and M. Frankignoulle (1999), Photosynthesis and calcification at cellular, organismal and community levels in coral reefs: A review on interactions and control by carbonate chemistry, *Amer. Zool.*, *39*(1), 160–183.

Grottoli, A. G. (2002), Effect of light and brine shrimp on skeletal $\delta^{13}C$ in the Hawaiian coral *Porites compressa*: A tank experiment, *Geochim. Cosmochim. Acta*, *66*(11), 1955–1967.

Grottoli, A. G., and G. M. Wellington (1999), Effect of light and zooplankton on skeletal $\delta^{13}C$ values in the eastern Pacific corals *Pavona clavus* and *Pavona gigantea*, *Coral Reefs*, *18*(1), 29–41.

Heikoop, J. M., J. J. Dunn, M. J. Risk, H. P. Schwarcz, T. A. McConnaughey, and I. M. Sandeman (2000), Separation of kinetic and metabolic isotope effects in carbon-13 records preserved in reef coral skeletons, *Geochim. Cosmochim. Acta*, *64*(6), 975–987.

Kaplan, A., M. A. Cane, Y. Kushnir, A. C. Clement, M. B. Blumenthal, and B. Rajagopalan (1998), Analyses of global sea surface temperature 1856–1991, *J. Geophys. Res.*, *103*(C9), 18,567–18,589, doi:10.1029/97JC01736.

Keeling, C. D. (1979), The Suess effect: ^{13}Carbon-^{14}carbon interrelations, *Environ. Int.*, *2*(4), 229–300.

Keeling, C. D., S. C. Piper, R. B. Bacastow, M. Wahlen, T. P. Whorf, M. Heimann, and H. A. Meijer (2001), *Exchanges of Atmospheric CO_2 and $^{13}CO_2$ with the Terrestrial Biosphere and Oceans from 1978 to 2000. I. Global Aspects*, *SIO Reference Series, No. 01–06*, 88 pp., Scripps Inst. of Oceanog., San Diego, Calif.

Knutson, D. W., S. V. Smith, and R. W. Buddemeier (1972), Coral chronometers: Seasonal growth bands in reef corals, *Science*, *177*(4045), 270–272.

Lamb, H. H. (1965), The Early Medieval Warm Epoch and its sequel, *Paleogeogr. Paleoclimatol. Paleoecol.*, *1*, 13–37.

Land, L. S., J. C. Lang, and B. N. Smith (1975), Preliminary observations on the carbon isotopic composition of some reef coral tissues and symbiotic zooxanthellae, *Limnol. Oceanogr.*, *20*(2), 283–287.

Land, L. S., J. C. Lang, and D. J. Barnes (1977), On the stable carbon and oxygen isotopic composition of some shallow water, ahermatypic, scleractinian coral skeletons, *Geochim. Cosmochim. Acta*, *41*(1), 169–172.

Leder, J. J., A. M. Szmant, and P. K. Swart (1991), The effect of prolonged "bleaching" on skeletal banding and stable isotopic composition in *Montastrea annularis*, *Coral Reefs*, *10*(1), 19–27.

Liu, Y., et al. (2014), Acceleration of modern acidification in the South China Sea driven by anthropogenic CO_2, *Sci. Rep.*, *4*, 5148.

Lough, J. M. (2010), Climate records from corals, *Wires Clim. Change*, *1*(3), 318–331.

Ludwig, K. R. (2003), Users Manual for Isoplot/Ex version 3.0: A Geochronological Toolkit for Microsoft Excel. Berkeley Geochronology Centre Special Publication No. 3.

Madonia, P., and J. Reitner (2014), Anthropogenic and solar forcing in $\delta^{13}C$ time pattern of coralline sponges, *Isot. Environ. Health Stud.*, *50*(4), 491–496.

Maier, C., J. Patzold, and R. P. M. Bak (2003), The skeletal isotopic composition as an indicator of ecological and physiological plasticity in the coral genus *Madracis*, *Coral Reefs*, *22*(4), 370–380.

Matthews, J. A., and K. R. Briffa (2005), The "Little Ice Age": Re-evalutaion of an evolving concept, *Geogr. Ann. Ser. A-Phys. Geogr.*, *87*(1), 17–36.

McConnaughey, T. A. (1989), ^{13}C and ^{18}O isotopic disequilibrium in biological carbonates: I. Patterns, *Geochim. Cosmochim. Acta*, *53*, 151–162.
McConnaughey, T. A. (2003), Sub-equilibrium oxygen-18 and carbon-13 levels in biological carbonates: Carbonate and kinetic models, *Coral Reefs*, *22*(4), 316–327.
McConnaughey, T. A., J. Burdett, J. F. Whelan, and C. H. Paull (1997), Carbon isotopes in biological carbonates: Respiration and photosynthesis, *Geochim. Cosmochim. Acta*, *61*(3), 611–622.
Moyer, R. P., and A. G. Grottoli (2011), Coral skeletal carbon isotopes ($\delta^{13}C$ and $\Delta^{14}C$) record the delivery of terrestrial carbon to the coastal waters of Puerto Rico, *Coral Reefs*, *30*(3), 791–802.
Pelejero, C., E. Calvo, M. T. McCulloch, J. F. Marshall, M. K. Gagan, J. M. Lough, and B. N. Opdyke (2005), Preindustrial to modern interdecadal variability in coral reef pH, *Science*, *309*(5744), 2204–2207.
Porter, J. W., W. K. Fitt, H. J. Spero, and C. S. Rogers (1989), Bleaching in reef corals: Physiological and stable isotopic responses, *Proc. Natl. Acad. Sci. U. S. A.*, *86*, 9342–9346.
Quinn, T. M., T. J. Crowley, F. W. Taylor, C. Henin, P. Joannot, and Y. Join (1998), A multicentury stable isotope record from a New Caledonia coral: Interannual and decadal sea surface temperature variability in the southwest Pacific since 1657 A.D, *Paleoceanography*, *13*(4), 412–426, doi:10.1029/98PA00401.
Reynaud, S., C. Ferrier-Pages, R. Sambrotto, A. Juillet-Leclerc, J. Jaubert, and J. P. Gattuso (2002), Effect of feeding on the carbon and oxygen isotopic composition in the tissues and skeleton of the zooxanthellate coral *Stylophora pistillata*, *Mar. Ecol.-Prog. Ser.*, *238*, 81–89.
Reynolds, R. W., N. A. Rayner, T. M. Smith, D. C. Stokes, and W. Wang (2002), An improved in situ and satellite SST analysis for climate, *J. Clim.*, *15*(13), 1609–1625.
Robock, A. (1979), The "Little Ice Age": Northern Hemisphere average observations and model calculations, *Science*, *206*(4425), 1402–1404.
Rosenfeld, M., R. Yam, A. Shemesh, and Y. Loya (2003), Implication of water depth on stable isotope composition and skeletal density banding patterns in a *Porites lutea* colony: Results from a long-term translocation experiment, *Coral Reefs*, *22*(4), 337–345.
Swart, P. K. (1983), Carbon and oxygen isotope fractionation in scleractinian corals: A review, *Earth-Sci. Rev.*, *19*(1), 51–80.
Swart, P. K., J. J. Leder, A. M. Szmant, and R. E. Dodge (1996), The origin of variations in the isotopic record of scleractinian corals: II. Carbon, *Geochim. Cosmochim. Acta*, *60*(15), 2871–2885.
Swart, P. K., L. Greer, B. E. Rosenheim, C. S. Moses, A. J. Waite, A. Winter, R. E. Dodge, and K. Helmle (2010), The ^{13}C Suess effect in scleractinian corals mirror changes in the anthropogenic CO_2 inventory of the surface oceans, *Geophys. Res. Lett.*, *37*, L05604, doi:10.1029/2009GL041397.
Vieira, L. E. A., S. K. Solanki, N. A. Krivova, and I. Usoskin (2011), Evolution of the solar irradiance during the Holocene, *Astron. Astrophys.*, *531*, A6.
Wang, C. Z., W. Q. Wang, D. X. Wang, and Q. Wang (2006), Interannual variability of the South China Sea associated with El Niño, *J. Geophys. Res.*, *111*, C03023, doi:10.1029/2005JC003333.
Watanabe, T., A. Winter, T. Oba, R. Anzai, and H. Ishioroshi (2002), Evaluation of the fidelity of isotope records as an environmental proxy in the coral *Montastraea*, *Coral Reefs*, *21*(2), 169–178.
Weber, J. N., P. Deines, P. H. Weber, and P. A. Baker (1976), Depth related changes in the $^{13}C/^{12}C$ ratio of skeletal carbonate deposited by the Caribbean reef-frame building coral *Montastrea annularis*: Further implications of a model for stable isotope fractionation by scleractinian corals, *Geochim. Cosmochim. Acta*, *40*, 31–39.
Wei, G. J., M. T. McCulloch, G. Mortimer, W. F. Deng, and L. H. Xie (2009), Evidence for ocean acidification in the Great Barrier Reef of Australia, *Geochim. Cosmochim. Acta*, *73*(8), 2332–2346.
Wei, G. J., Z. B. Wang, T. Ke, Y. Liu, W. F. Deng, X. F. Chen, J. F. Xu, T. Zeng, and L. H. Xie (2015), Decadal variability in seawater pH in the West Pacific: Evidence from coral $\delta^{11}B$ records, *J. Geophys. Res. Oceans*, *120*, 7166–7181, doi:10.1002/2015JC011066.
Weil, S. M., R. W. Buddemeier, S. V. Smith, and P. M. Kroopnick (1981), The stable isotopic composition of coral skeletons: Control by environmental variables, *Geochim. Cosmochim. Acta*, *45*(7), 1147–1153.
Wu, W., W. Tan, L. Zhou, H. Yang, and Y. Xu (2012), Sea surface temperature variability in southern Okinawa Trough during last 2700 years, *Geophys. Res. Lett.*, *39*, L14705, doi:10.1029/2012GL052749.